

**Supplementary information for:**

**Structure and characterization of phosphoglucomutase 5 from herring - an inactive enzyme with intact substrate binding**

**Robert Gustafsson<sup>1,†</sup>, Ulrich Eckhard<sup>1, †,‡</sup>, Weihua Ye<sup>2</sup>, Erik D. Enbody<sup>2</sup>, Mats Pettersson<sup>2</sup>, Per Jemth<sup>2</sup>, Leif Andersson<sup>2,3,4</sup> and Maria Selmer<sup>1,\*</sup>**

<sup>1</sup> Department of Cell and Molecular Biology, Uppsala University, BMC, Box 596, SE-751 24 Uppsala, Sweden; robert.gustafsson@icm.uu.se (R.G.); ueccri@ibmb.csic.es (U.E.)

<sup>2</sup> Department of Medical Biochemistry and Microbiology, Uppsala University, BMC, Box 582, SE-751 23 Uppsala, Sweden; weihua.ye@imbim.uu.se (W.Y.); erik.enbody@imbim.uu.se (E.D.E.); mats.pettersson@imbim.uu.se (M.P.); per.jemth@imbim.uu.se (P.J.); Leif.Andersson@imbim.uu.se (L.A.)

<sup>3</sup> Department of Veterinary Integrative Biosciences, Texas A&M University, College Station, TX 77843, USA

<sup>4</sup> Department of Animal Breeding and Genetics, Swedish University of Agricultural Sciences, SE-75007 Uppsala, Sweden

\* Correspondence: maria.selmer@icm.uu.se

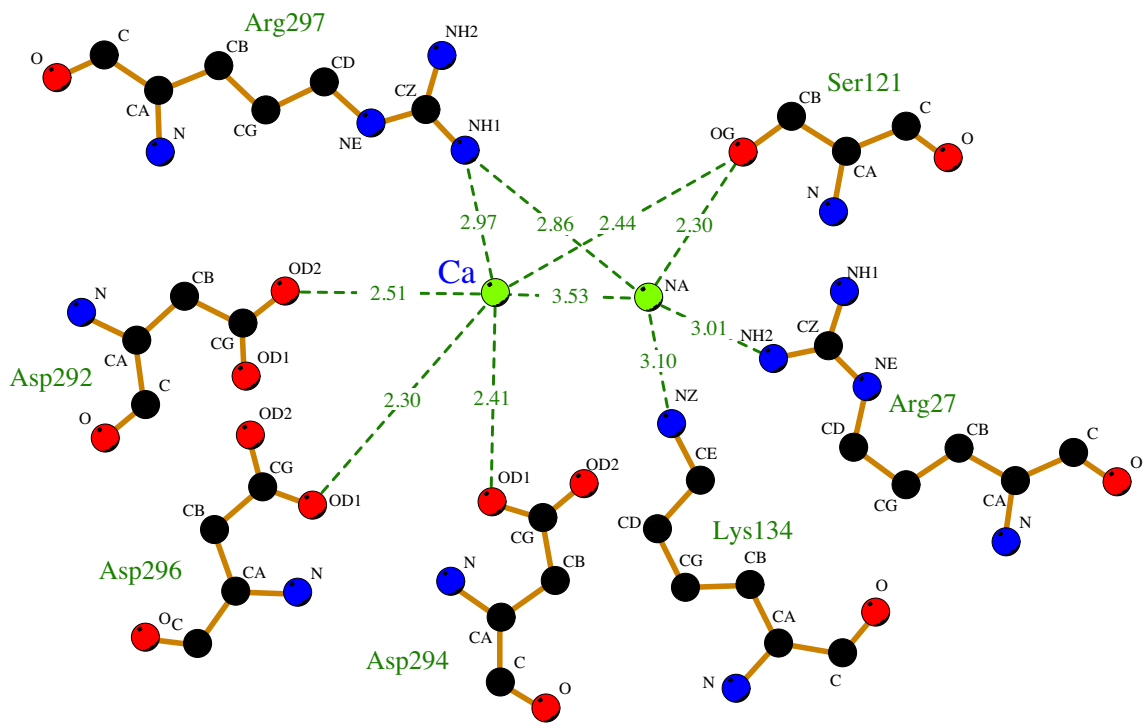
† These authors contributed equally.

‡ Current address: Proteolysis Lab, Department of Structural Biology, Molecular Biology Institute of Barcelona, CSIC, Barcelona Science Park, Baldiri Reixac, 15-21, 08028 Barcelona, Catalonia, Spain

**Content:**

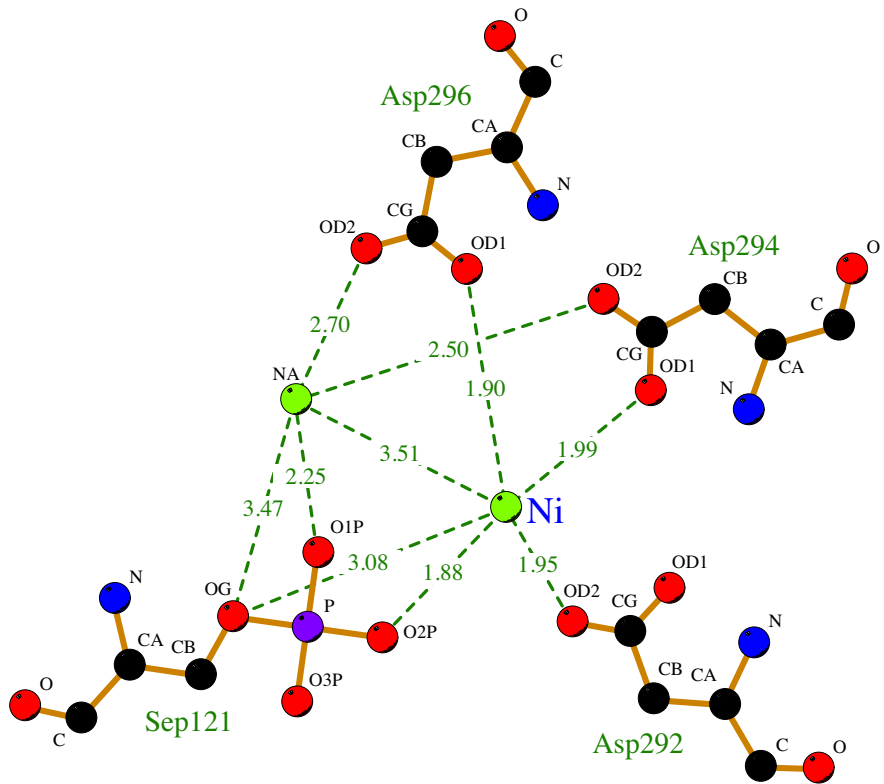
**Figure S1-S8**

**Table S1-S5**



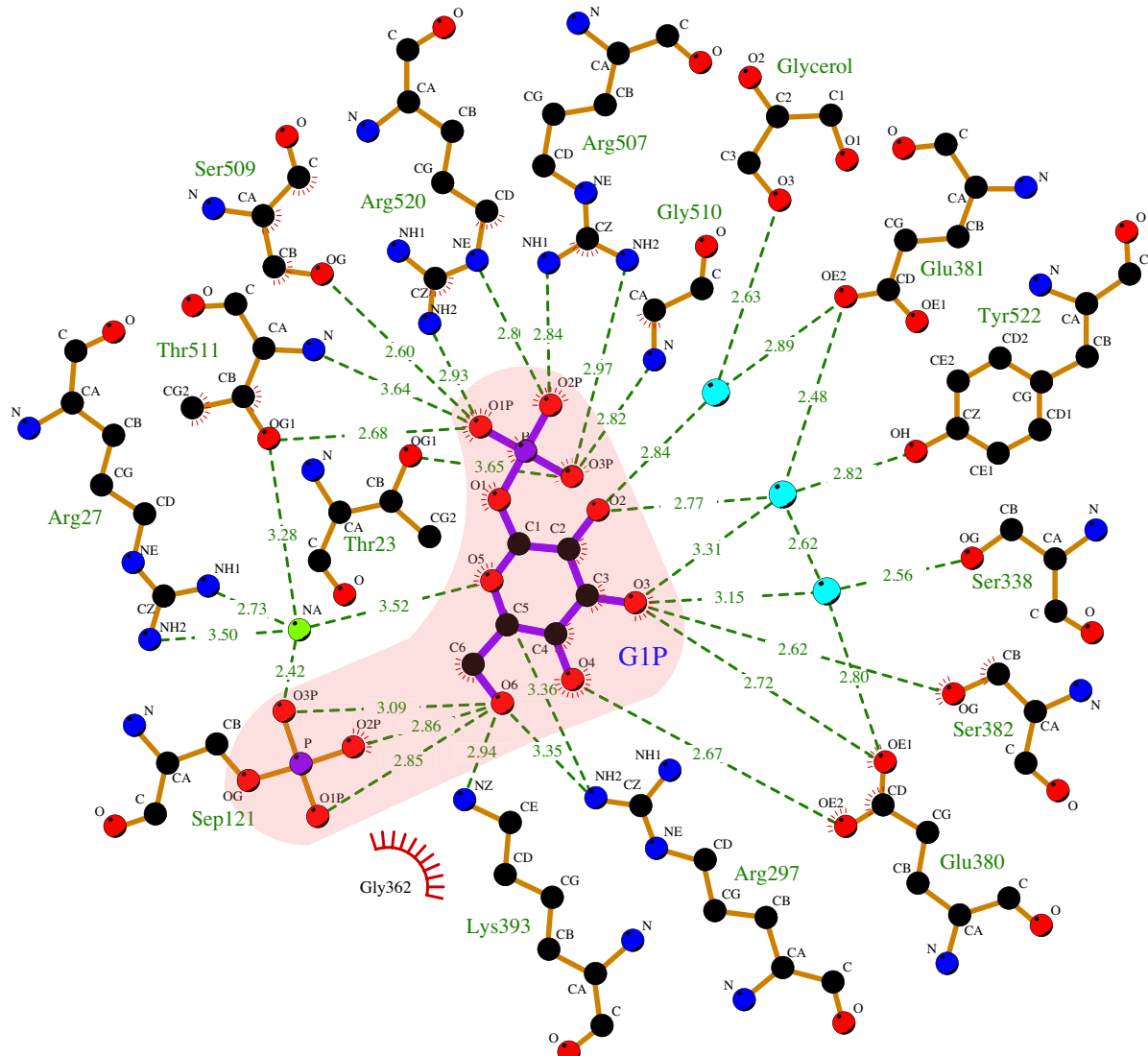
Ca bound to aPGM5

**Figure S1: Coordination of  $\text{Ca}^{2+}$  in apo aPGM5.**  $\text{Ca}^{2+}$  and aPGM5 residues are labelled blue and green, respectively. Green dashed lines indicate hydrogen bonds or electrostatic interactions, with distances indicated.  $\text{Ca}^{2+}$  and sodium ion are shown as green spheres. Figure prepared using LigPlot+ [1].



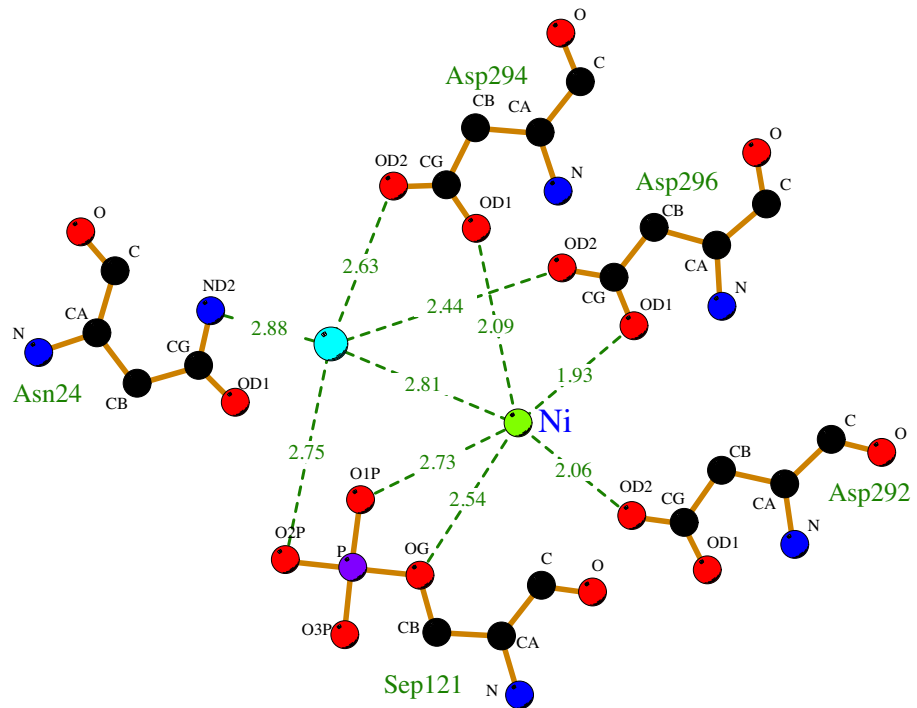
## Ni bound to bPGM5 apo

**Figure S2: Coordination of Ni<sup>2+</sup> in apo bPGM5.** Ni<sup>2+</sup> and bPGM5 residues are labelled blue and green, respectively. Green dashed lines indicate hydrogen bonds or electrostatic interactions, with distances indicated. Ni<sup>2+</sup> and sodium ion are shown as green spheres. Figure prepared using LigPlot+ [1].



G1P bound to bPGM5

**Figure S3: Coordination of G1P in bPGM5.** G1P and bPGM5 residues are labelled blue and green, respectively. Green dashed lines indicate hydrogen bonds or electrostatic interactions, with distances indicated. Residues or atoms involved in hydrophobic interactions are represented by an arc with spokes radiating towards the binding partners they contact. Bridging waters are shown as blue spheres, and sodium ion shown as green sphere. Figure prepared using LigPlot+ [1].



### Ni bound to bPGM5

**Figure S4: Coordination of  $\text{Ni}^{2+}$  in the bPGM5 G1P complex.**  $\text{Ni}^{2+}$  and bPGM5 residues are labelled blue and green, respectively. Green dashed lines indicate hydrogen bonds or electrostatic interactions, with distances indicated. Bridging water is shown as blue sphere. Figure prepared using LigPlot+ [1].

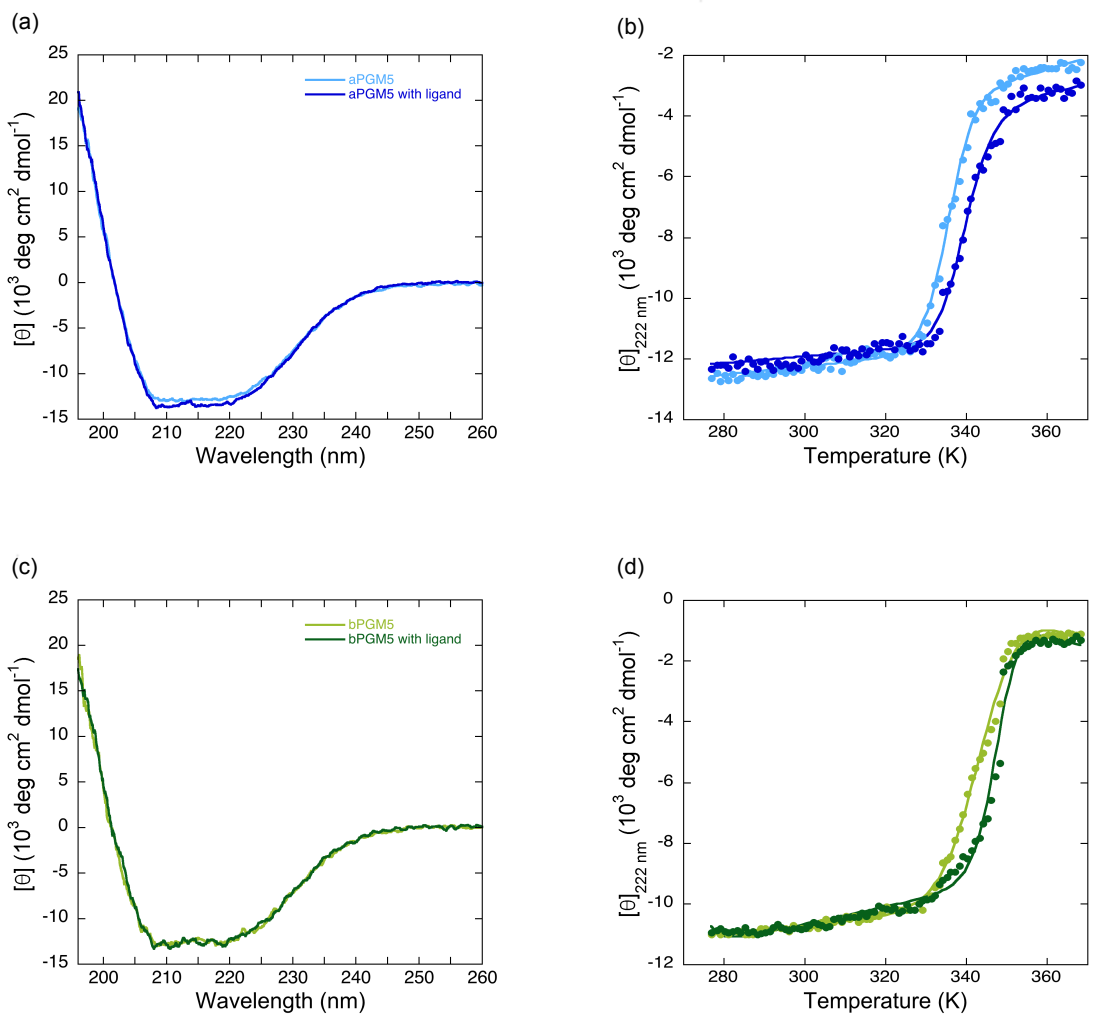


**Figure S5: CD spectroscopy measurements.** CD spectroscopy measurements for aPGM5 ((a) and (b), blue) and bPGM5 ((c) and (d), green) in the absence of ligand (light color) and in the presence of ligand, 0.5 mM G16P (dark color). ((a) and (c)) Representative CD spectra for aPGM5 (a) and bPGM5 (c) at 25 °C. ((b) and (d)) Representative thermal denaturation curves for aPGM5 (b) and bPGM5 (d) monitored at 222 nm and the  $T_m$  values are 336 K (aPGM5 apo), 340 K (aPGM5 with ligand), 342 K (bPGM5 apo) and 346 K (bPGM5 with ligand), respectively.

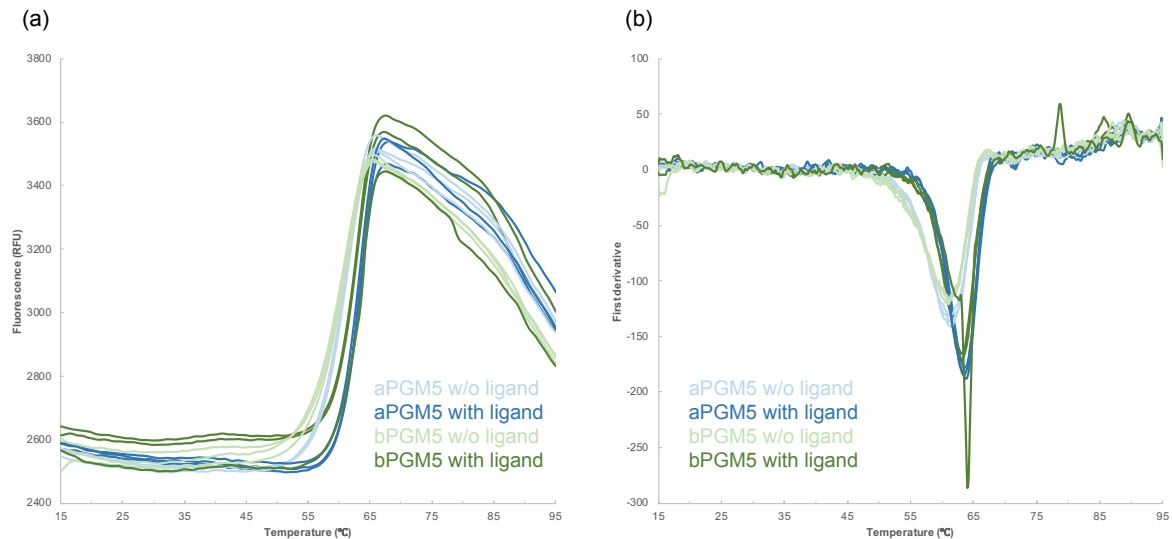


**Figure S6: DSF data.** DSF melting curves **(a)** and first derivative **(b)** for aPGM5 (blue) and bPGM5 (green) without His6-tag, measured without (light color) and in presence of (dark color) 500  $\mu$ M reaction intermediate G16P.

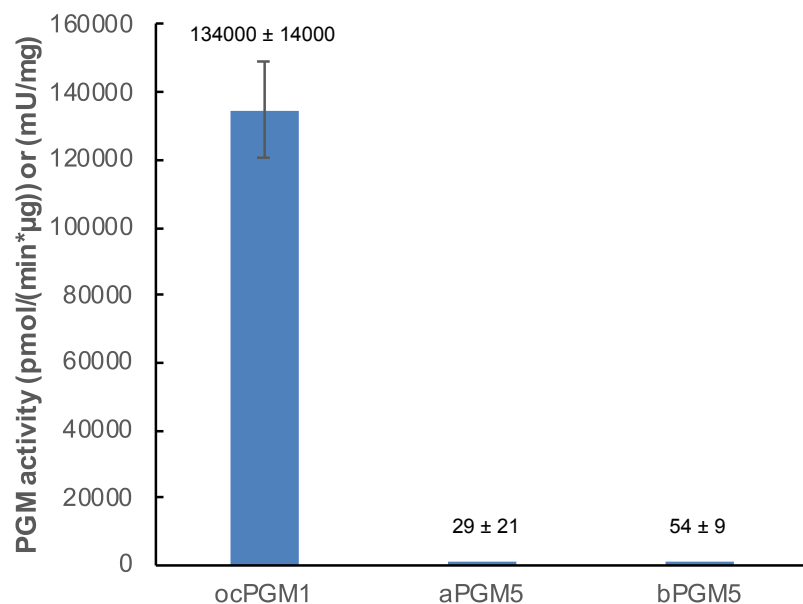


**Figure S7: Enzymatic activity data.** Phosphoglucomutase activity assay of positive control rabbit muscle PGM1 (ocPGM1), aPGM5 and bPGM5 in presence of MgCl<sub>2</sub> and G16P. Results are shown as average with error bars of +/- one standard deviation from triplicate experiments after subtraction of background activity. Background activity was measured without addition of substrate.

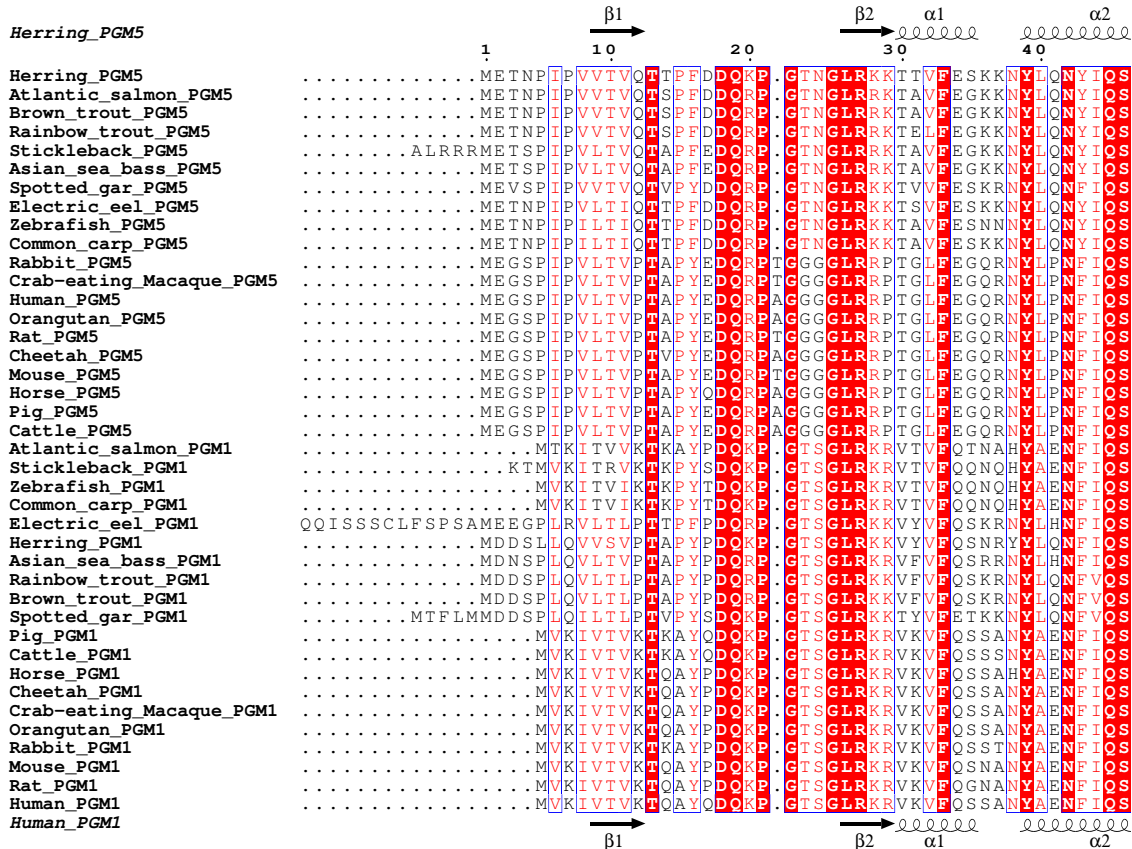
**Figure S8: Multiple sequence alignment of PGM5 and PGM1 from 10 fish species and 10 mammals.** The alignment was done using Clustal Omega and visualized using ESPript [2].

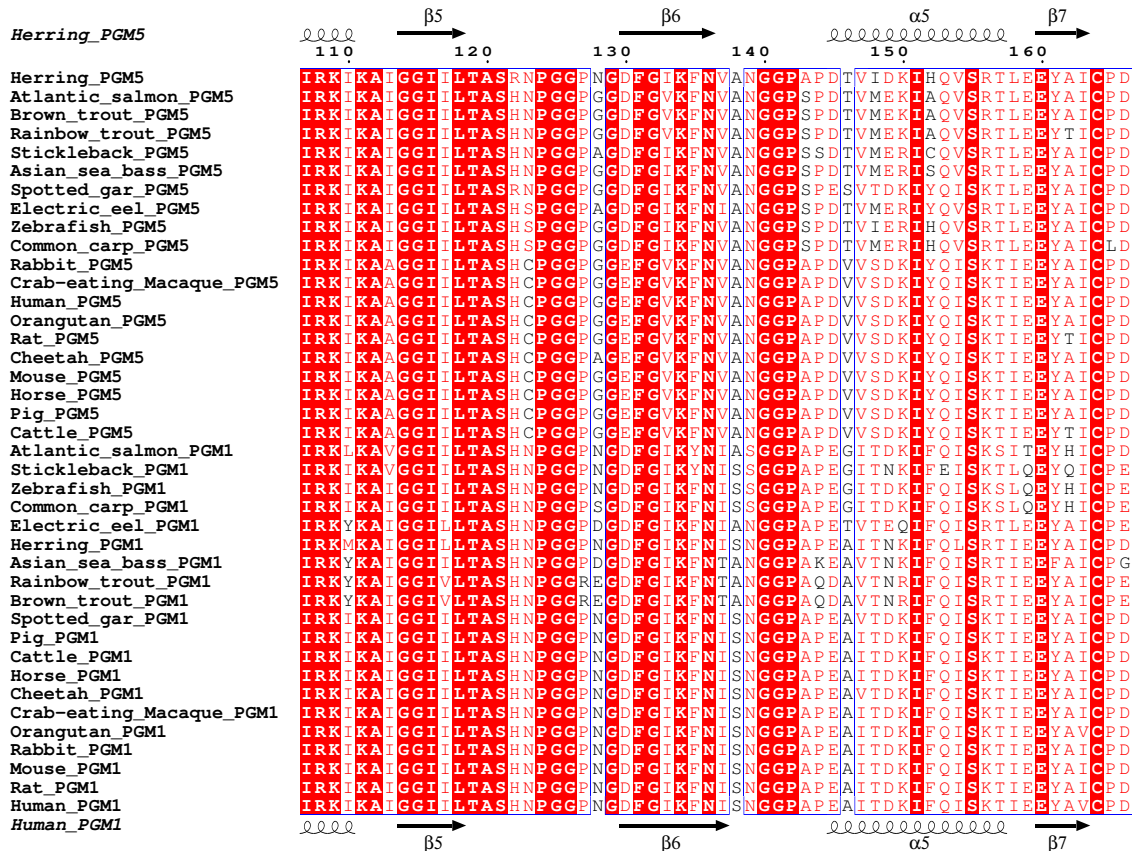
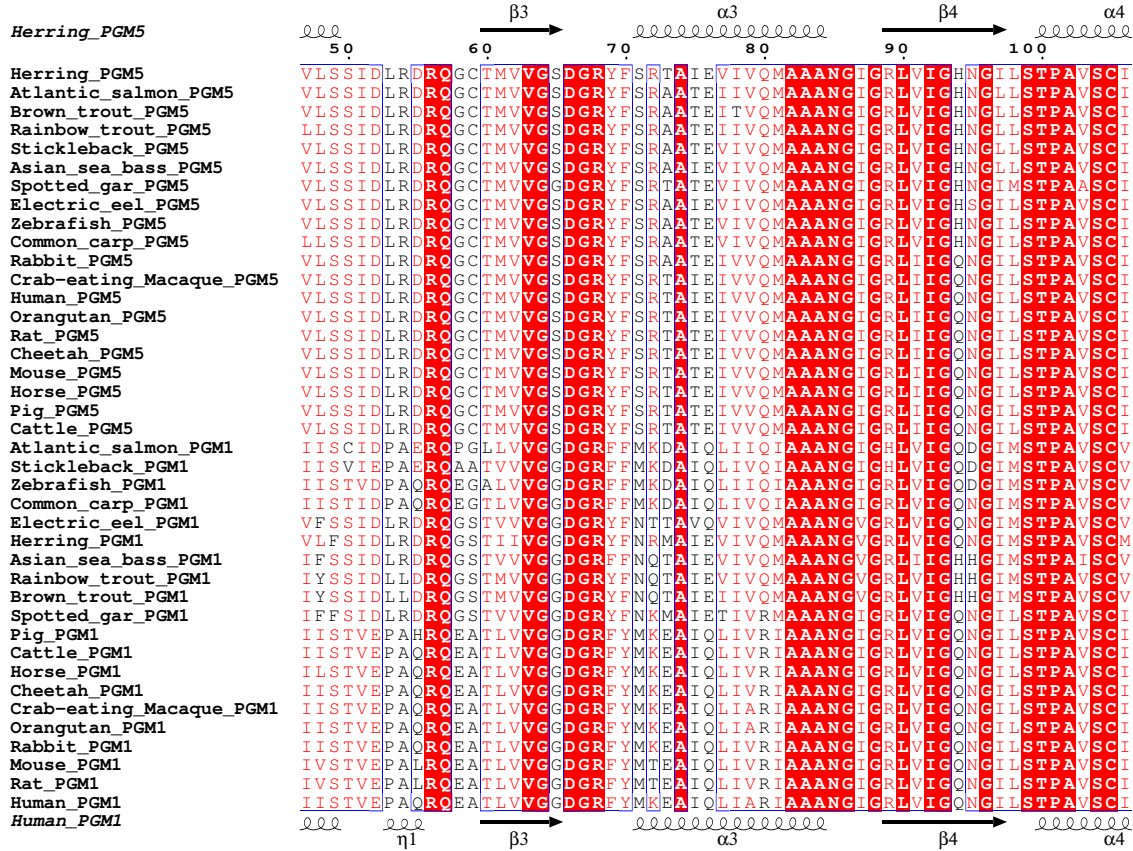
*Herring\_PGM5*

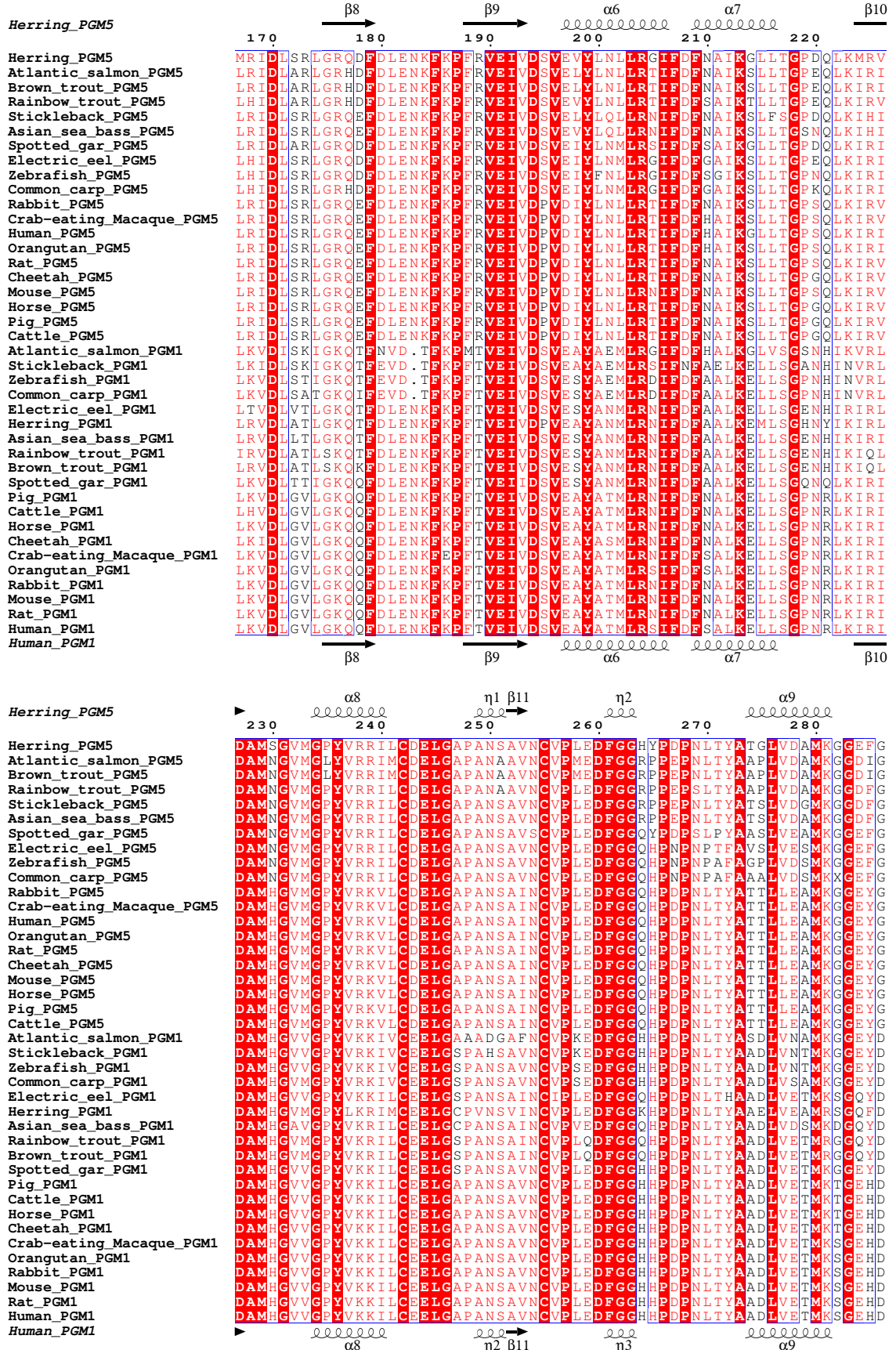
```

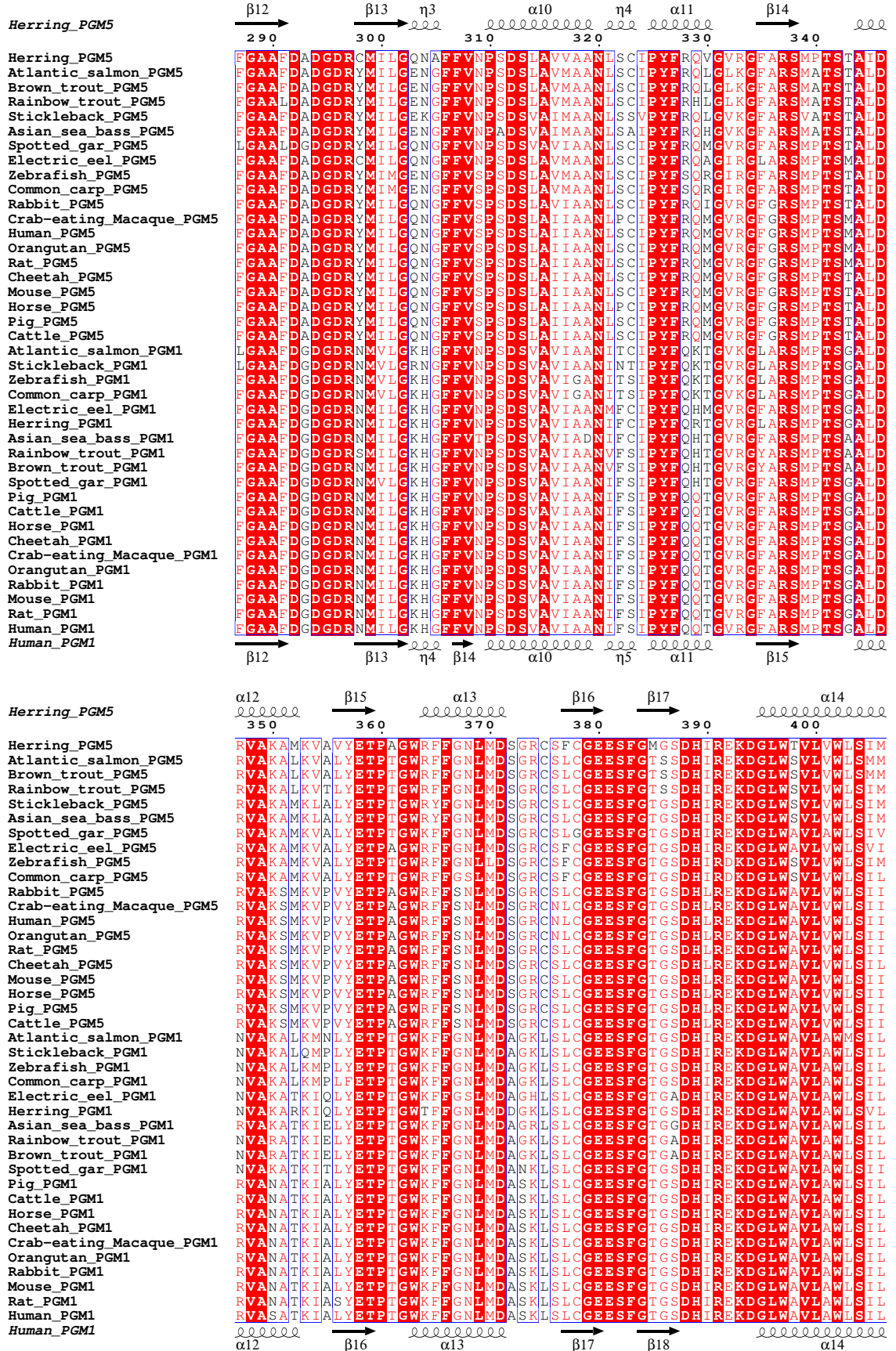
Herring_PGM5
Atlantic_salmon_PGM5
Brown_trout_PGM5
Rainbow_trout_PGM5
Stickleback_PGM5
Asian_sea_bass_PGM5
Spotted_gar_PGM5
Electric_eel_PGM5
Zebrafish_PGM5
Common_carp_PGM5
Rabbit_PGM5
Crab-eating_Macaque_PGM5
Human_PGM5
Orangutan_PGM5
Rat_PGM5
Cheetah_PGM5
Mouse_PGM5
Horse_PGM5
Pig_PGM5
Cattle_PGM5
Atlantic_salmon_PGM1
Stickleback_PGM1
Zebrafish_PGM1
Common_carp_PGM1
Electric_eel_PGM1
Herring_PGM1
Asian_sea_bass_PGM1
Rainbow_trout_PGM1
Brown_trout_PGM1
Spotted_gar_PGM1
Pig_PGM1
Cattle_PGM1
Horse_PGM1
Cheetah_PGM1
Crab-eating_Macaque_PGM1
Orangutan_PGM1
Rabbit_PGM1
Mouse_PGM1
Rat_PGM1
Human_PGM1
Human_PGM1

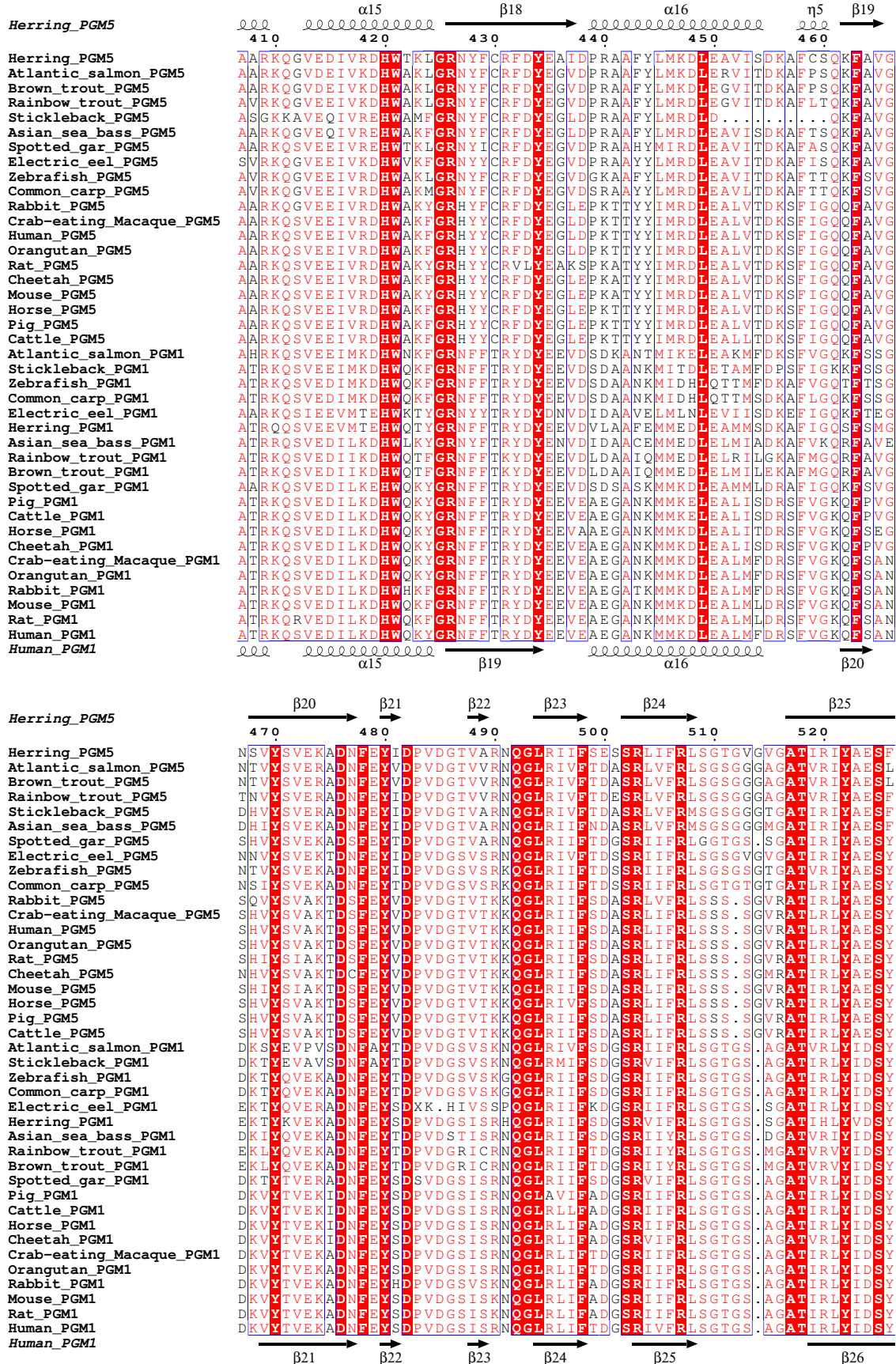
```











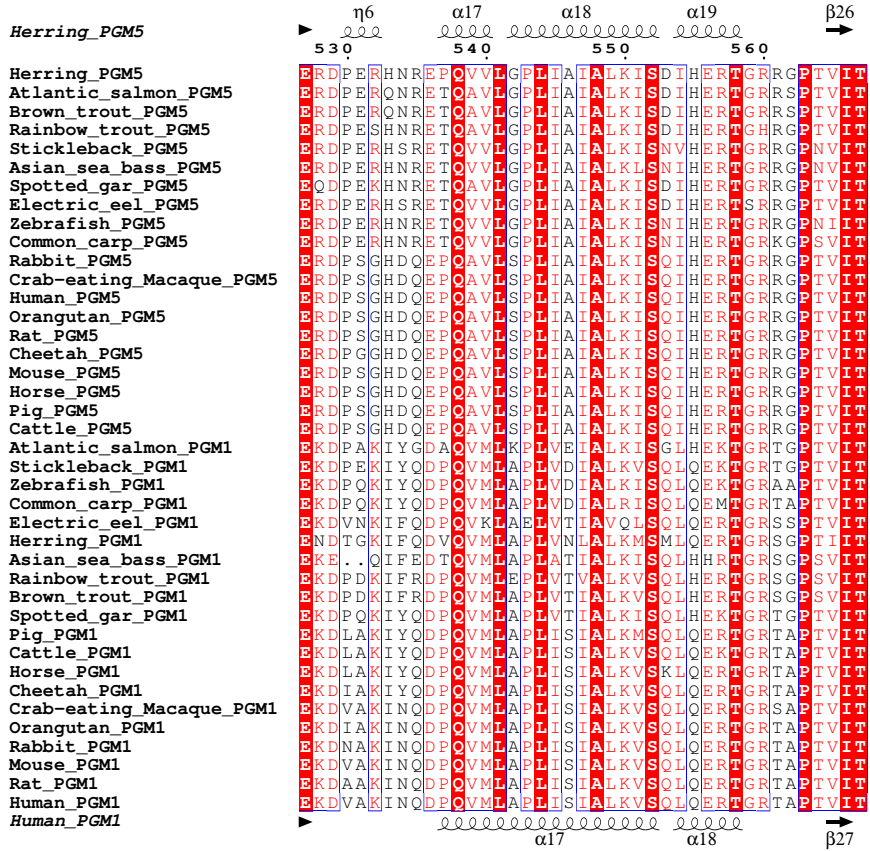


**Table S1:** List of localities for herring samples included in this study. Spawning season, latitude (lat), longitude (lon), salinity and allele frequency differences at SNPs in the vicinity of the PGM Ala330Val mutation (rs5164711).

The data are based on the previous study by Han et al. (<https://www.biorxiv.org/content/10.1101/2020.07.15.204214v1>) [3].

Identifier	Sample	Location	Spawning		Salinity (ppt)	Frequency of PGM5 SNP						Frequency of non-PGM5 SNP	
			season	lat		rs5164711	rs5178679	rs5178707	rs5181659	rs5181660	rs5199622	rs5218152	
1	A_Kalix_Baltic_Spring	Kalix	Spring	65,52	22,43	3	0,75	0,94	0,92	1,00	1,00	1	1
2	HGS1_Riga_Baltic_Spring	Gulf of Riga	Spring	58,34	24,62	5,5	0,84	0,91	0,93	1,00	1,00	1	0,98
3	HGS2_Riga_Baltic_Spring	Gulf of Riga	Spring	58,34	24,62	5,5	0,83	0,95	0,96	1,00	1,00	1	1
4	HGS3_Riga_Baltic_Autumn	Gulf of Riga	Autumn	58,1	23,92	5,5	0,65	0,73	0,75	1,00	0,97	0,75	0,84
5	HGS4_Riga_Baltic_Autumn	Gulf of Riga	Autumn	58,1	23,92	5,5	0,68	0,61	0,71	0,98	1,00	0,84	0,81
7	B_Vaxholm_Baltic_Spring	Vaxholm	Spring	59,26	18,18	6	0,71	0,84	0,92	1,00	1,00	1	1
8	PB1_Hästskär_Baltic_Spring	Hästskär	Spring	60,35	17,48	6	0,89	0,96	0,94	1,00	1,00	1	1
9	PB4_Hudiksvall_Baltic_Spring	Hudiksvall	Spring	61,45	17,3	6	0,87	0,98	1,00	1,00	1,00	0,97	1
10	PB5_Gävle_Baltic_Spring	Gävle	Spring	60,43	17,18	6	0,87	0,83	0,96	1,00	1,00	1	1
6	PB6_Gävle_Baltic_Summer	Gävle	Summer	60,43	17,18	6	0,90	0,95	0,95	1,00	1,00	1	1
11	PB7_Gävle_Baltic_Autumn	Gävle	Autumn	60,44	17,35	6	0,74	0,67	0,81	1,00	1,00	0,85	0,87
12	G_Gamleby_Baltic_Spring	Gamleby	Spring	57,5	16,27	7	0,82	0,94	0,95	1,00	1,00	1	1
13	PB11_Kalmar_Baltic_Spring	Kalmar	Spring	57,39	17,07	7	0,78	0,90	0,91	1,00	1,00	1	1
14	PB12_Karlskrona_Baltic_Spring	Karlskrona	Spring	56,1	15,33	7	0,87	0,92	0,92	1,00	1,00	1	0,97
19	HGS12_BornholmBasin_Baltic_Autumn	Bornholm Basin	Autumn	55,3	15,22	8	0,68	0,71	0,77	1,00	1,00	0,64	0,86
15	HGS71_Rugen_Baltic_Spring	Rügen	Spring	54,14	13,47	8	0,68	0,92	1,00	1,00	1,00	1	1
16	HGS72_Rugen_Baltic_Spring	Rügen	Spring	54,14	13,47	8	0,80	0,84	0,90	1,00	1,00	1	0,96
17	PN3_CentralBaltic_Baltic_Spring	Central Baltic	Spring	55,24	15,51	8	0,88	0,84	0,96	1,00	1,00	0,97	1
18	TysklandS18_Germany_Baltic	Ariadnegrund	Spring	54,22	13,58	8	0,76	0,97	0,98	1,00	1,00	1	1
21	HGS5_Schlei_Baltic_Autumn	Schlei	Autumn	54,6	9,76	9	0,69	1,00	1,00	1,00	0,96	1	1
20	HGS6_Schlei_Baltic_Spring	Schlei	Spring	54,6	9,76	9	0,67	0,74	0,80	1,00	0,97	0,93	0,89
23	HGS11_RingkobingFjord_NorthSea_Spring	Ringkobing Fjord	Spring	56,02	8,19	12	0,83	0,81	0,83	1,00	1,00	0,96	0,95
22	H_Fehmarn_Baltic_Autumn	Fehmarn	Autumn	54,5	11,3	12	0,62	0,77	0,80	0,98	0,98	0,66	0,79
24	HGS24_Landvik_Atlantic_Spring	Landvik	Spring	58,32	8,5	15	0,39	0,32	0,53	0,96	0,98	0,58	0,57
25	LandvikS17_Atlantic_Spring	Landvik	Spring	58,32	8,5	15	0,26	0,22	0,37	1,00	0,84	0,43	0,52
26	J_Traslovslage_Baltic_Spring	Träslövsläge	Spring	57,03	12,11	20	0,70	0,77	0,78	1,00	0,97	0,66	0,92
27	PB9_Kattegat_Atlantic_Spring	Kattegat, Björköfjorden	Spring	57,43	11,42	23	0,62	0,57	0,64	0,94	0,98	0,5	0,51
29	HGS8_KattegatNorth_Atlantic_Spring	Kattegat North	Spring	57,4	11,4	25	0,23	0,13	0,26	1,00	0,90	0,11	0,07

28	O_Hamburgsund_Atlantic_Spring	Hamburgsund	Spring	58,3	11,13	25	0,34	0,16	0,33	0,96	0,98	0,14	0,09
30	PB10_Skagerrak_Atlantic_Spring	Skagerrak, Brofjorden	Spring	58,19	11,21	25	0,23	0,12	0,35	1,00	1,00	0,15	0,26
31	HGS25_Lindas_Atlantic_Spring	Lindås	Spring	60,73	5,13	28	0,12	0,02	0,27	1,00	0,98	0,03	0,04
32	HGS26_Lusterfjorden_Atlantic_Spring	Lusterfjorden	Spring	61,48	7,58	32	0,15	0,00	0,33	1,00	0,97	0	0
34	HGS17_IsleOfMan_IrishSea_Autumn	Douglas Bank, Isle of Man	Autumn	54,06	-4,37	33	0,07	0,00	0,30	0,98	1,00	0	0,03
33	HGS23_Clyde_Atlantic_Spring	Ballantrae, Clyde	Spring	55,14	-5,04	33	0,03	0,02	0,24	1,00	0,97	0	0,04
35	HGS19_TeelinBay_Atlantic_Winter	Teelin Bay	Winter	54,63	-8,63	34	0,04	0,00	0,32	0,98	0,98	0	0
48	DalBoB_Atlantic_Autumn	Bonavista Bay	Autumn	48,49	-53,2	35	0,15	0,00	0,30	0,95	1,00	0	0
38	DalFB_Atlantic_Spring	Fortune Bay	Mixed	47,17	-55,38	35	0,11	0,00	0,34	0,71	0,98	0	NA
49	DalGeB_Atlantic_Autumn	German Banks	Autumn	43,16	-66,18	35	0,07	0,04	0,20	0,98	0,93	0	0
39	DalInB_Atlantic_Spring	Inner Baie Des Chaleurs	Spring	48	-65,51	35	0,13	0,00	0,43	0,96	1,00	0	0
50	DalNsF_Atlantic_Autumn	Northumberland Strait	Autumn	45,44	-62,36	35	0,16	0,00	0,29	1,00	1,00	0	0
40	DalNsS_Atlantic_Spring	Northumberland Strait	Spring	46,19	-64,09	35	0,07	0,00	0,26	0,93	0,98	0	0
36	HGS10_Downs_EnglishChannel_Winter	Downs	Winter	51,34	1,9	35	0,15	0,02	0,26	0,96	0,98	0	0,03
41	HGS15_NSSH_Atlantic_Spring	Norway	Spring	67,46	9,47	35	0,10	0,00	0,31	0,92	1,00	0	0
51	HGS16_Orkney_NorthSea_Autumn	Orkney	Autumn	59	-2	35	0,07	0,00	0,16	1,00	0,97	0	0
47	HGS18_CelticSea_Atlantic_AutumnWinter	Celtic Sea	Winter	51,59	-6,51	35	0,08	0,07	0,17	0,98	1,00	0	0
42	HGS20_CapeWrath_Atlantic_Spring	Isle of Skye	Spring	57,41	-6,13	35	0,08	0,00	0,23	0,98	0,98	0	0
46	HGS21_Hebrides_Atlantic_Mixed	West of Hebrides	Mixed	58,17	-7,23	35	0,10	0,00	0,18	1,00	0,95	0	0
52	HGS22_CapeWrath_Atlantic_Autumn	Cape Wrath	Autumn	58,61	-4,37	35	0,08	0,00	0,25	0,87	0,91	0	0
43	HGS27_Gloppen_Atlantic_Spring	Gloppen	Spring	61,77	6,16	35	0,13	0,03	0,27	1,00	1,00	0	0
37	HGS9_Greenland_Atlantic_Spring	Greenland	Summer	60,78	-47,15	35	0,13	0,00	0,03	0,93	0,98	0	0
53	N_NorthSea_Atlantic_Autumn	North Sea	Autumn	58,06	6,1	35	0,03	0,00	0,25	0,98	1,00	0	0
45	PB2_Iceland_Atlantic_Spring	Iceland, Höfn	Spring	65,49	-12,58	35	0,11	0,00	0,42	0,89	0,93	0	0
P	PB8_Pacific_Pacific_Spring	Vancouver, Strait of Georgia	Spring	NA	NA	35	0,00	0,00	0,00	1,00	0,96	0	0
44	Q_Norway_Atlantic_Atlantic_Spring	Norway	Spring	64,52	10,15	35	0,16	0,00	0,24	0,95	0,98	0	0

**Table S2:** Sequences of transcripts for PGM5 predicted from ENSEMBL-provided annotation of the herring genome

>ENSCHAT00000060054	MCKRYSAFDEYDYRPLRGTSFHQLTTPFDDQKPGTNGLRKKTTVFESKKNYLQNYIQSVLSSIDLDRQGCTMVGSDGRYFSRTAIEVIVQMAAANGIGRLVIGHNGILSTPAVSCIIRKIKAIIGGIILTASRNPGGPNDFGIKFNVANGGPAPDTVIDKIHQVSRTLEEYAICPDMRIDLSRLGRQDFDLENKFKPFRVEIVDSVEVYLNLLRGIFDFNAIKGLLTGPDQLKMRVDAMSGVMGPYVRRILCDELGAPANSAVNCVPLEDFGGHYPDPNLTYATGLVDAMKGGEFGFGAAFDADGDRCMILGQNAFFVNPSDSLAVVAANLSCIPYFRQGVVRGFARSMPSTAIDRVAKAMKVAVYETPAGWRFFGNLMDSGRCSFCGEESFGMGS DHIREKDGLWTVLVWL SIMAARKQGVEDIVRDHWTKLGRNYFCRFDYEAI DPRAAFYLMKDLEAVISDKAFCSQKFAVGNSVYSVEKADNFYIDPV DGTVARNQGLRIIFSESSRLIFRLSGTGVGVGATIRIYAESFERDPERHNREPQVVLGPLIAIALKISDIHERTRGGPTVIT
>ENSCHAT00000060060	YEVYREFLSATIAKTNPIP VVTVQTTPFDDQKPGTNGLRKKTTVFESKKNYLQNYIQSVLSSIDLDRQGCTMVGSDGRYFSRTAIEVIVQMAAANGIGRLVIGHNGILSTPAVSCIIRKIKAIIGGIILTASRNPGGPNDFGIKFNVANGGPAPDTVIDKIHQVSRTLEEYAICPDMRIDLSRLGRQDFDLENKFKPFRVEIVDSVEVYLNLLRGIFDFNAIKGLLTGPDQLKMRVDAMSGVMGPYVRRILCDELGAPANSAVNCVPLEDFGGHYPDPNLTYATGLVDAMKGGEFGFGAAFDADGDRCMILGQNAFFVNPSDSLAVVAANLSCIPYFRQGVVRGFARSMPSTAIDRVAKAMKVAVYETPAGWRFFGNLMDSGRCSFCGEESFGMGS DHIREKDGLWTVLVWL SIMAARKQGVEDIVRDHWTKLGRNYFCRFDYEAI DPRAAFYLMKDLEAVISDKAFCSQKFAVGNSVYSVEKADNFYIDPV DGTVARNQGLRIIFSESSRLIFRLSGTGVGVGATIRIYAESFERDPERHNREPQVVLGPLIAIALKISDIHERTRGGPTVIT
>ENSCHAT00000060079	METNPPIP VVTVQTTPFDDQKPGTNGLRKKTTVFESKKNYLQNYIQSVLSSIDLDRQGCTMVGSDGRYFSRTAIEVIVQMAAANGIGRLVIGHNGILSTPAVSCIIRKIKAIIGGIILTASRNPGGPNDFGIKFNVANGGPAPDTVIDKIHQVSRTLEEYAICPDMRIDLSRLGRQDFDLENKFKPFRVEIVDSVEVYLNLLRGIFDFNAIKGLLTGPDQLKMRVDAMSGVMGPYVRRILCDELGAPANSAVNCVPLEDFGGHYPDPNLTYATGLVDAMKGGEFGFGAAFDADGDRCMILGQNAFFVNPSDSLAVVAANLSCIPYFRQGVVRGFARSMPSTAIDRVAKAMKVAVYETPAGWRFFGNLMDSGRCSFCGEESFGMGS DHIREKDGLWTVLVWL SIMAARKQGVEDIVRDHWTKLGRNYFCRFDYEAI DPRAAFYLMKDLEAVISDKAFCSQKFAVGNSVYSVEKADNFYIDPV DGTVARNQGLRIIFSESSRLIFRLSGTGVGVGATIRIYAESFERDPERHNREPQVVLGPLIAIALKISDIHERTRGGPTRRAFTKCRVLFFSFFYYCYYFNISRHH
>ENSCHAT00000060097	METNPPIP VVTVQTTPFDDQKPGTNGLRKKTTVFESKKNYLQNYIQSVLSSIDLDRQGCTMVGSDGRYFSRTAIEVIVQMAAANGIGRLVIGHNGILSTPAV

	CIIRKIKAIIGGIILTASRNPGGPNDFGIKFNVANGGPAPDTVIDKIHQVSR TLEEYAICPDMRIDLSRLGRQDFDLENKFKPFRVEIVDSVEVYLNLLRGIFD FNAIKGLLTGPDQLKMRVDAMSGVMGPYVRRILCDELGAPANSAVNCVPLED FGGHYPDPNLTYATGLVDAMKGGEFGFGAAFDADGDRCMILGQNAFFVNPSD SLAVVAANLSCIPYFRQVGVRGFARSMPSTAIDRVAKAMKVAVYETPAGWR FFGNLMDSGRCSFCGEESFGMGSDHIREKDGLWTVLVWLSIMAARKQGVEDI VRDHWTKLGRNYFCRFDYEAIIDPRAAFYLMKDLEAVISDKAFCSQKFAVGNS VYSVEKADNFYEYIDPVDTGTVARNQGLRIIFSESSRLIFRLSGTGVGVGATIR IYAESFERDPERHNREPQVQDTTLTGLSSSFSSSSASFSSSFVHTASPDY FAQMSESKTTQFMN
--	--

**Table S3:** Sequences of aPGM5 and bPGM5 used in this manuscript

>pNIC28-Bsa4_aPGM5_AlA330_Atlantic_aa	>pNIC28-Bsa4_bPGM5_Val330_Baltic_aa
MHHHHHHSSGVDLGTENLYFQ↓S METNPIPVVTVQTPFDDQKPGTNGLRKTTVFES KKNYLQNYIQSVLSSIDLDRDQGCTMVVGSDGRYF SRATAIEVIVQMAAANGIGRLVIGHNGILSTPAVSC IIRKIKAIIGGIILTASRNPGGPNGDFGIKFNVANG GPAPDTVIDKIHQVSRTLEEYAICPDMRIDLSRLG RQDFDLENKFKPFRVEIVDSVEVYLNLRGIFDFN AIKGLLTGPDQLKMRVDAMSGVMGPYVRRILCDEL GAPANSAVNCVPLEDFGGHYPDPNLTYATGLVDAM KGGEFGFGAAFDADGDRCMILGQNAFFVNPSDSL VVAANLSCIPIYFRQ <b>A</b> GVRGFARSMPTSTAIDRVAK AMKVAVYETPAGWRFFGNLMDSGRCSCGEESFGM GSDHIREKDGLWTVLWLSIMAARKQGVEDIVRDH WTKLGRNYFCRFDYEAIDPRAAFYLMKDLEAVISD KAFCSQKFAVGNSVYSVEKADNFYIDPVDTV NQGLRIIFSESSRLIFRLSGTGVGVGATIRIYAES FERDPERHNREPQVVLGPLIAIALKISDIHERTGR RGPTVIT*	MHHHHHHSSGVDLGTENLYFQ↓S METNPIPVVTVQTPFDDQKPGTNGLRKTTVFES KKNYLQNYIQSVLSSIDLDRDQGCTMVVGSDGRYF SRATAIEVIVQMAAANGIGRLVIGHNGILSTPAVSC IIRKIKAIIGGIILTASRNPGGPNGDFGIKFNVANG GPAPDTVIDKIHQVSRTLEEYAICPDMRIDLSRLG RQDFDLENKFKPFRVEIVDSVEVYLNLRGIFDFN AIKGLLTGPDQLKMRVDAMSGVMGPYVRRILCDEL GAPANSAVNCVPLEDFGGHYPDPNLTYATGLVDAM KGGEFGFGAAFDADGDRCMILGQNAFFVNPSDSL VVAANLSCIPIYFRQ <b>V</b> GVRGFARSMPTSTAIDRVAK AMKVAVYETPAGWRFFGNLMDSGRCSCGEESFGM GSDHIREKDGLWTVLWLSIMAARKQGVEDIVRDH WTKLGRNYFCRFDYEAIDPRAAFYLMKDLEAVISD KAFCSQKFAVGNSVYSVEKADNFYIDPVDTV NQGLRIIFSESSRLIFRLSGTGVGVGATIRIYAES FERDPERHNREPQVVLGPLIAIALKISDIHERTGR RGPTVIT*

**Table S4:** RMSD values from pairwise structure comparison using PDBeFOLD [4]. hsPGM1-2 = human PGM1 isoform 2.

Structure	PDB code	Chain	aPGM5 apo <b>6Y8X, Chain A</b> RMSD (Å) (aligned C $\alpha$ atoms)	bPGM5 apo <b>6Y8Z, Chain A</b> RMSD (Å) (aligned C $\alpha$ atoms)	bPGM5 + G-1-P <b>6Y8Y, Chain A</b> RMSD (Å) (aligned C $\alpha$ atoms)
<b>aPGM5 apo</b>	6Y8X	A	0	0.641 (545)	0.610 (547)
<b>bPGM5 apo</b>	6Y8Z	A	0.641 (545)	0	0.267 (567)
<b>bPGM5 + G-1-P</b>	6Y8Y	A	0.610 (547)	0.267 (567)	0
<b>hsPGM1 apo</b>	5EPC	A	1.872 (532)	1.538 (540)	1.656 (540)
<b>hsPGM1 apo</b>	5EPC	B	1.663 (529)	1.362 (539)	1.473 (536)
<b>hsPGM1 + G-6-P</b>	6BJ0	A	1.789 (533)	1.464 (540)	1.591 (542)
<b>hsPGM1 + G-6-P</b>	6BJ0	B	1.721 (534)	1.378 (540)	1.508 (544)
<b>ocPGM1 apo</b>	3PMG	A	1.582 (481)	1.893 (527)	1.654 (505)
<b>ocPGM1 apo</b>	3PMG	B	1.899 (538)	1.514 (543)	1.645 (545)
<b>ptPGM + sulfate</b>	1KFI	A	1.187 (522)	1.169 (531)	1.181 (534)
<b>ptPGM + sulfate</b>	1KFI	B	1.748 (520)	1.493 (525)	1.634 (530)
<b>ptPGM apo</b>	1KFQ	A	1.845 (467)	1.911 (493)	1.891 (484)
<b>ptPGM apo</b>	1KFQ	B	1.716 (477)	1.831 (503)	1.872 (499)
<b>hsPGM1-2 apo</b>	6SNP	A	1.304 (530)	1.064 (539)	1.139 (537)
<b>hsPGM1-2 + G-1-P</b>	6SNO	A	1.307 (534)	1.000 (540)	1.074 (544)
<b>hsPGM1-2 + G-6-P</b>	6SNQ	A	1.366 (523)	1.109 (539)	1.188 (539)
<b>ocPGM1 + G-1-P-6-V *</b>	1C4G	A	1.100 (465)	1.285 (491)	1.284 (487)
<b>ocPGM1 + G-1-P-6-V *</b>	1C4G	B	1.960 (517)	1.664 (534)	1.802 (536)
<b>ocPGM1 + G-1,6-BP *</b>	1C47	A	1.542 (495)	1.733 (530)	1.550 (511)
<b>ocPGM1 + G-1,6-BP *</b>	1C47	B	1.932 (529)	1.593 (533)	1.706 (533)

\* Structures have serious errors in placement of domain 4.

**Table S5:** Details of sequences included in Figure S8. The query coverage was 98-100%.

Species common name	Species latin name	PGM1 from species			PGM5 from species		
		Accession code UniProt or GenBank	Sequence identity to bPGM5 (%)	Sequence identity to hsPGM1 (%)	Accession code UniProt or GenBank	Sequence identity to bPGM5 (%)	Sequence identity to hsPGM1 (%)
Herring (baltic)	<i>Clupea harengus (membras)</i>	XP_01267 3001.1	67.7	76.3	XP_01267 6095.1	100	67.6
Zebrafish	<i>Danio rerio</i>	F1QF00	64.1	82.0	B0R0B3	86.2	66.4
Stickleback	<i>Gasterosteus aculeatus</i>	G3NVH9	63.0	79.9	G3NVP3	82.7	63.4
Spotted gar	<i>Lepisosteus oculatus</i>	XP_00663 4913.2	70.7	83.8	W5MSS7	85.4	70.4
Common carp	<i>Cyprinus carpio</i>	XP_01895 0613.1	65.1	81.1	XP_01897 7408.1	85.4	65.8
Atlantic salmon	<i>Salmo salar</i>	B5DG72	62.9	77.9	A0A1S3P FY1	85.71	64.8
Rainbow trout	<i>Oncorhynchus mykiss</i>	XP_02146 8451.1	68.3	75.2	XP_02147 7693.1	85.2	64.2
Electric eel	<i>Electrophorus electricus</i>	XP_02685 4191.1	66.8	74.2	XP_02687 0188.1	87.3	66.7
Brown trout	<i>Salmo trutta</i>	XP_02955 9985.1	68.3	75.9	XP_02957 2366.1	85.5	65.6
Asian sea bass / barramundi	<i>Lates calcarifer</i>	XP_01853 2842.1	68.8	76.3	XP_01852 5124.1	86.8	65.1
Human	<i>Homo sapiens</i>	P36871	67.6	100	Q15124	78.7	65.1
Rabbit	<i>Oryctolagus cuniculus</i>	P00949	68.3	97.0	G1T6S2	79.23	65.8
Mouse	<i>Mus musculus</i>	Q9D0F9	68.2	97.3	Q8BZF8	78.9	65.1

Sumatran Orangutan	<i>Pongo abelii</i>	K7EU15	67.8	99.3	A0A2J8X HD5	78.5	65.1
Crab-eating Macaque	<i>Macaca fascicularis</i>	Q4R5E4	67.8	98.8	A0A2K5V RN8	78.5	65.0
Horse	<i>Equus caballus</i>	F6X8Q2	68.3	96.4	F7DQ57	78.7	65.3
Cheetah	<i>Acinonyx jubatus</i>	XP_02691 4801.1	68.9	96.1	XP_02689 6886.1	79.2	65.5
Pig	<i>Sus scrofa</i>	F1S814	68.3	96.1	F1SJE6	79.1	65.3
Cattle	<i>Bos taurus</i>	Q08DP0	68.2	96.1	A6QNJ7	78.9	65.1
Rat	<i>Rates norvegicus</i>	P38652	68.0	96.6	D3ZVR9	78.4	64.6
Ciliate PGM	<i>Paramecium tetraurelia</i>	P47244	47.0	50.5			
Human (isoform 2)	<i>Homo sapiens</i>	P36871-2	69.7	93.1			

## REFERENCES

1. Laskowski, R.A.; Swindells, M.B. LigPlot+: multiple ligand-protein interaction diagrams for drug discovery. *J Chem Inf Model* **2011**, *51*, 2778–2786, doi:10.1021/ci200227u.
2. Robert, X.; Gouet, P. Deciphering key features in protein structures with the new ENDscript server. *Nucleic Acids Res.* **2014**, *42*, W320-4, doi:10.1093/nar/gku316.
3. Han, F.; Jamsandekar, M.; Pettersson, M.E.; Su, L.; Fuentes-Pardo, A.; Davis, B.; Bekkevold, D.; Berg, F.; Cassini, M.; Dahle, G.; et al. The genetic architecture underlying ecological adaptation in Atlantic herring is not consistent with the infinitesimal model. *bioRxiv* **2020**, 2020.07.15.204214, doi:10.1101/2020.07.15.204214.
4. Krissinel, E.; Henrick, K. Secondary-structure matching (SSM), a new tool for fast protein structure alignment in three dimensions. *Acta Crystallogr. Sect. D Biol. Crystallogr.* **2004**, *60*, 2256–2268, doi:10.1107/S0907444904026460.